S. Afr. J. Chem., 2012, **65**, 150–158,
<http://journals.sabinet.co.za/sajchem/>.

Spectral and Thermal Characterization and Antimicrobial Effect of 3-(5-H/Me/Cl/NO_2-1*H*-benzimidazol-2-yl)-benzene-1,2-diols and Some Transition Metal Complexes

Aydin Tavman[a,], A. Seher Birteksoz[b] and Faruk Oksuzomer[c]

[a]*Istanbul University, Faculty of Engineering, Department of Chemistry, 34320, Avcilar, Istanbul, Turkey.*

[b]*Istanbul University, Faculty of Pharmacy, Department of Pharmaceutical Microbiology, 34452, Beyazit, Istanbul, Turkey.*

[c]*Istanbul University, Faculty of Engineering, Department of Chemical Engineering, 34320, Avc lar, Istanbul, Turkey.*

Submitted 20 April 201 revised 28 May 2012, accepted 4 June 2012.

ABSTRACT

3-(5-H/Me/Cl/NO_2-1*H*-benzimidazol-2-yl)-benzene-1,2-diols (HL_X; X = 1–4) ligands and HL_3 complexes with $Fe(NO_3)_3$, $Cu(NO_3)_2$, $Co(NO_3)_2$, $Zn(NO_3)_2$ have been synthesized and characterized. The structural representations of the compounds are proposed on the basis of elemental analysis, molar conductivity, TGA, mass, FT-IR, ^{1}H- and ^{13}C-NMR spectrometry. All of the complexes are 1:1 electrolyte and have 1:1 M:L ratio except that of Cu(II).All of the complexes present fluorescence, the Co(II) complex showing the highest fluorescence intensity and the highest emission wavelength in comparison to the other complexes. Antibacterial activities of the ligands and the complexes formed by the HL_3 ligand were evaluated using the disk diffusion method against six bacteria and *Candida albicans.* HL_1, HL_2, HL_3 and $[Cu(\mathbf{HL_3})(\mathbf{L_3})(H_2O)_2](NO_3)\cdot H_2O$ show considerable antimicrobial activity toward *S. epidermidis* and *C. albicans.*

KEYWORDS

Benzimidazole, benzene-1,2-diol, metal complexes, antimicrobial activity, fluorescence spectroscopy.

1. Introduction

Benzimidazolyl-phenol ligands are known to be strong chelating agents. These ligands are potential N,O donors and they react easily with metal ions to give stable chelate complexes. Various transition metal chelate complexes of benzimidazolyl-phenol type ligands have been reported.[1–15]

In our previous studies, a series of benzimidazolyl-phenol ligands and their metal complexes were synthesized, and their antimicrobial activities were investigated. For example, 2-methoxy-6-(5-H/methyl/chloro/nitro-1*H*-benzimidazol-2-yl)-phenol ligands and some transition metal complexes were synthesized and characterized. Some of the mentioned ligands, and Cu(II) and Zn(II) complexes showed antibacterial activity against Gram+ bacteria.[16] It has also been reported that 4-methoxy-2-(1*H*-benzimidazol-2-yl)-phenol and the corresponding Ag(I) and Cu(II) complexes are effective on *S. epidermidis, S. aureus* and *B. subtilis.* Also, 4-methoxy-2-(5-methyl/chloro-1*H*-benzimidazol-2-yl)-phenols showed antibacterial activity toward *S. aureus.*[17] While 2-methyl-6-(1*H*-benzimidazol-2-yl)-phenol had no activity, the corresponding Ag(I) and Zn(II) complexes showed antibacterial activity toward *K. pneumoniae, S. epidermidis* and *S. aureus* bacteria.[18] 2-(5-Nitro-1*H*-benzimidazol-2-yl)-4-bromophenol and their Cu(II) and Fe(III) complexes showed considerable antibacterial activity against *S. epidermidis* relative to Ciprofloxazin.[19] 2-(5-H/Me/Cl-1*H*-benzimidazol-2-yl)-phenols, 2-(5-H/Me-1*H*-benzimidazol-2-yl) -4-bromo/nitro-phenols and their Fe(III) and Zn(II) complexes showed broad-spectrum (Gram+ and Gram– bacteria) activity.[13,20,21]

In this work, 3-(5-H/methyl/chloro/nitro-1*H*-benzimidazol-2-yl)-benzene-1,2-diols (HL_X; X = 1–4) ligands (Fig. 1) and the (Fe(III), Cu(II), Co(II) and Zn(II) complexes with 3-(5-chloro-1*H*-benzimidazol-2-yl)-benzene-1,2-diol (HL_3) are reported. Herein, we discuss the characterizations of the compounds and the structural–biological activity relationship of the ligands and the complexes.

* To whom correspondence should be addressed. E-mail: atavman@istanbul.edu.tr

2. Experimental

All chemicals and solvents were reagent grade and were used as purchased without further purification. Melting points were determined using an Electrothermal melting-point apparatus. Analytical data were obtained with a Thermo Finnigan Flash EA 1112 analyzer. Molar conductivities of the complexes were measured on a WTW Cond315i conductivity meter in dimethyl sulfoxide (DMSO) at 25 °C. ^{1}H- and ^{13}C-NMR spectra were recorded on a Varian Unity Inova 500 NMR spectrometer. The residual DMSO-d_6 signal was used as an internal reference. Solid FT-IR spectra were recorded using KBr disks on a Mattson 1000 FT-IR spectrometer. The electron spray ionization (ESI) MS analyses were carried out in positive ion modes using a Thermo Finnigan LCQ Advantage MAX LC/MS/MS. Thermogravimetric (TG) analyses were made on a TG-60WS Shimadzu, with a heating rate of 10 °C min^{-1} under flowing air at the rate of 50 mL min^{-1}.

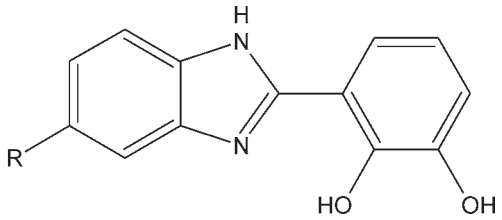

Figure 1 Structural representation of the ligands.
R = H, HL_1; R = CH_3, HL_2; R = Cl, HL_3; R = NO_2, HL_4

Magnetic measurements were carried out on a Sherwood Scientific apparatus (MK1) at room temperature using Gouy's method. Fluorescence spectra were performed on a Shimadzu RF-5301 PC Spectrofluorophotometer.

2.1. Synthesis of the Ligands: General Procedure

The ligands were prepared according to literature procedures.[7,22] For instance, 3-(5-chloro-1*H*-benzimidazol-2-yl)-benzene-1,2-diol (HL_3) was obtained by reaction of 2,3-dihydroxybenzaldehyde (1.38 g, 10 mmol) and the equivalent amount of $NaHSO_3$ (1.04 g, 10 mmol) at room temperature in 25 mL ethanol for 4–5 h. The mixture was treated with 4-chloro-1,2-phenylenediamine (1.43 g, 10 mmol) in 15 mL dimethylformamide and gently refluxed for 2 h. The reaction mixture was then poured into 500 mL icy water, filtered and crystallized from ethanol.

2.2. Synthesis of the Complexes

2.2.1. *[Fe(**L**$_3$)(OH)(H$_2$O)$_3$](NO$_3$)*

131 mg of HL_3 (0.502 mmol) in ethanol (10 mL) was treated with 202 mg $Fe(NO_3)_3{\cdot}9H_2O$ (0.500 mmol) in ethanol (5 mL) at ~60 °C for 2 h. The solution mixture was allowed to stand at ~4 °C for several days, until a black solid product precipitated, which was collected by filtration and dried under vacuum over $CaCl_2$.

2.2.2. *[Co(**L**$_3$)(H$_2$O)$_2$](NO$_3$)*

131 mg of HL_3 (0.502 mmol) and 146 mg of $Co(NO_3)_2{\cdot}6H_2O$ (0.502 mmol) were reacted in ethanol (10 mL). After 8 h reflux the black precipitate was filtered and dried under vacuum over $CaCl_2$.

2.2.3. *[Cu(**HL**$_3$)(**L**$_3$)(H$_2$O)$_2$](NO$_3$)·H$_2$O*

131 mg of HL_3 (0.502 mmol) and 121 mg of $Cu(NO_3)_2{\cdot}3H_2O$ (0.501 mmol) were reacted in ethanol (10 mL). After 4 h reflux the brown precipitate was filtered and dried under vacuum over $CaCl_2$.

2.2.4. *[Zn(**L**$_3$)(H$_2$O)$_2$](NO$_3$)*

131 mg of HL_3 (0.502 mmol) were suspended in ethyl acetate (10 mL), and 149 mg of $Zn(NO_3)_2{\cdot}6H_2O$ (0.501 mmol) in ethylacetate (5 mL) was added to the ligand suspension. The mixture was refluxed for 2 h. The brown precipitate was filtered and dried under vacuum over $CaCl_2$.

2.3. Determination of Antimicrobial Activity

Antimicrobial activity against *Staphylococcus aureus ATCC 6538, Staphylococcus epidermidis ATCC 12228, Escherichia coli ATCC 8739, Klebsiella pneumoniae ATCC 4352, Pseudomonas aeruginosa ATCC 27853, Proteus mirabilis ATCC 14153* and *Candida albicans ATCC 10231* were determined by the micro broth dilutions technique strictly following the National Committee for Clinical Laboratory Standards (NCCLS) recommendations.[23,24] Mueller-Hinton broth for bacteria, RPMI-1640 medium, buffered to pH 7.0 with MOPS for yeast strain was used as the test medium. Serial two-fold dilutions ranging from 5000 μg mL^{-1} to 4.9 μg mL^{-1} were prepared. The inoculum was prepared using a 4–6 h broth culture of each bacteria and 24 cultures of yeast strains adjusted to a turbidity equivalent to a 0.5 McFarland standard, diluted in broth media to give a final concentration of 5×10^5 cfu mL^{-1} for bacteria and 0.5×10^3 to 2.5×10^3 cfu mL^{-1} for yeast in the test tray. The trays were covered and placed in plastic bags to prevent evaporation. The trays containing Mueller-Hinton broth were incubated at 35 °C for 18–20 h and the trays containing RPMI-1640 medium were incubated at 35 °C for 46–50 h. The minimum inhibitory concentrations (MIC) were defined as the lowest concentration of compound giving complete inhibition of visible growth. Ciprofloxacin and sodium cefuroxime were used as reference antimicrobials for bacteria and yeast, respectively. As control, antimicrobial effect of solvent (DMSO) was investigated against test microorganisms.

3. Results and Discussion

3.1. Physical Properties

The analytical data and physical properties of the ligands and the complexes are summarized in Table 1.

All the complexes are quite stable and could be stored for months without any appreciable change. The complexes do not have sharp melting points but decompose above 350 °C.

The molar conductivity values of the complexes are 32, 34, 42 and 43 Ω^{-1} cm^2 mol^{-1} for the Fe(III), Co(II),Cu(II) and Zn(II) complexes, respectively. These results are indicative of 1:1 electrolyte complexes.

It is known that the solvent plays a considerable role in complexation.[25,26] In this study, Fe(III) and Cu(II) easily complexed with HL_3 whereas Co(II) was able to complex at the end of an 8 h period. All the reactions were done in ethanol. However, Zn(II) did not complex with the ligand in ethanol, due to the strong intramolecular hydrogen bonding between the OH hydrogen and C = N nitrogen atom present in the ligand. This fact can be explained as follows: Zn(II) ion is a borderline Lewis acid, and it cannot overcome the intramolecular hydrogen bonding and the complex cannot form. Therefore, the complexation reaction of HL_3 with Zn(II) occurs with a high yield in ethyl acetate because of the good solubility of both the ligand and $Zn(NO_3)_2{\cdot}6H_2O$ in it.

3.2. Magnetic Moments

The room temperature magnetic moment value of [Fe(**L**$_3$)(OH)(H$_2$O)$_3$](NO$_3$) complex is 3.90 BM, which is lower than the spin only value ~5.90 BM for Fe(III) d^5 with S = 5/2 (high spin under a weak crystal field) and higher than the spin only value of ~2.0 BM in the case of S = 1/2 (low spin in the presence of a strong crystal field). The intermediate values of the magnetic moment indicate stabilization of the species having intermediate ferric spin (S = 3/2) state for this complex.[27,28]

The magnetic moment value of the Cu(II) complex is 1.86 BM, which is in the expected range for mononuclear d^9 (e.g. Cu^{2+}) complexes.

The observed magnetic moment value for the Co(II) complex, 4.38 BM, lies in the range reported for tetrahedral Co(II) complexes having three unpaired electrons.[29] This value is high for that of three unpaired electrons (3.87 BM). The electronic configuration of a tetrahedral Co(II) complex is $(d_{x^2-y^2})^2 (d_{z^2})^2 (d_{xy})^1 (d_{yz})^1 (d_{xz})^1$. It is known that both tetrahedral and high-spin octahedral Co(II) complexes possess three unpaired electrons but may be distinguished by the magnitude of the deviation of μ_{eff} from the spin-only value. The magnetic moment of tetrahedral Co(II) complexes with an orbitally nongenerate ground term is increased above the spin-only value *via* contribution from higher orbitally degenerate terms and occurs in the range 4.2–4.7 BM.[30]

3.3. FT-IR Spectra

FT-IR spectral data of the ligands and the complexes are given in Table 2. The characteristic ν(O–H) and ν(N–H) vibration frequencies of the ligands exhibit strong or medium bands at *ca.* 3400 and 3300 cm^{-1}, respectively.[20,31,32] These bands change

Table 1 The analytical data and physical properties of HL_1–HL_4 and the complexes.

Compound	Found (calcd) %			Yield %	M.p.(dec.) [a]	Λ [b]	Colour
	C	H	N				
HL_1 $C_{13}H_{10}N_2O_2$	68.8 (69.0)	4.7 (4.5)	12.1 (12.4)	62	225	–	Colourless
HL_2 $C_{14}H_{12}N_2O_2$	70.3 (70.0)	5.3 (5.0)	11.4 (11.7)	66	182	–	Colourless
HL_3 $C_{13}H_9ClN_2O_2$	59.9 (59.9)	3.7 (3.5)	10.4 (10.7)	71	221	–	Light yellow
HL_4 $C_{13}H_9N_3O_4$	57.4 (57.6)	3.5 (3.3)	15.5 (15.5)	58	323	–	Yellow
$[Fe(\mathbf{L_3})(OH)(H_2O)_3](NO_3)$ [c] $C_{13}H_{15}ClFeN_3O_9$	35.3 (34.8)	3.1 (3.4)	9.0 (9.4)	75	>350	32	Black
$[Co(\mathbf{L_3})(H_2O)_2](NO_3)$ [c] $C_{13}H_{12}ClCoN_3O_7$	37.8 (37.5)	3.3 (2.9)	10.4 (10.1)	70	>350	34	Black
$[Cu(\mathbf{HL_3})(\mathbf{L_3})(H_2O)_2](NO_3)$ [c] $\cdot H_2O$; $C_{26}H_{22}Cl_2CuN_5O_{10}$	45.0 (44.7)	3.6 (3.3)	10.4 (10.0)	67	>350	42	Brown
$[Zn(\mathbf{L_3})(H_2O)_2](NO_3)$ $C_{13}H_{12}ClN_3O_7Zn$	37.3 (36.9)	3.2 (2.9)	9.9 (9.9)	85	>350	43	Brown

[a] dec., decomposed, °C.
[b] Λ, molar conductivity, Ω^{-1} cm^2 mol^{-1} (25 °C).
[c] μ_{eff} values for Fe(III), Cu(II) and Co(II) complexes are 3.90, 1.86 and 4.38 BM, respectively.

significantly upon metal complexation indicating deprotonation and subsequent involvement of the phenoxyl group in metal coordination. The phenolic oxygen atom coordination is supported by the appearance of medium bands at a lower frequency region *ca.* 500 cm^{-1}, assignable to ν(M–OC) vibration frequencies.[33]

Appearance of the broad bands above 3400 cm^{-1} in the complexes may be due to the ν(N–H) (and stretching of uncoordinated water molecules for Cu(II) complex) vibration frequencies. The characteristic ν(C–H) and δ(C–H) modes of ring residues and aliphatic groups (methyl and methoxy) are observed in the wavenumber region between 3200–2940 cm^{-1} and 900–700 cm^{-1} (Table 2). The ν(C = C) frequencies for the ring residue are expected to appear at *ca.* 1630 cm^{-1} with their own characteristics for the ligands in the IR spectra. Similarly the (C = N) asymmetric stretching frequencies are expected to appear at *ca.* 1600 cm^{-1}. This IR band is observed at 1591 cm^{-1} in HL_3 ligand and shifts to higher frequencies in the complexes. This shift may support the argument that coordination occurs *via* the imine nitrogen atom.

Intra- or intermolecular H-bonding was observed in the IR spectra of the ligands, between 2900–2500 cm^{-1} as broad bands. The sequence of intramolecular hydrogen bonding from the strongest to the weakest was: $HL_4 > HL_3 > HL_2 \approx HL_1$. HL_4 was expected to have the strongest H-bonding because of the nitro group.

All of the complexes show strong bands at *ca.* 1385 cm^{-1} in their IR spectra, supporting the presence of uncoordinated nitrate ion, which was also confirmed by conductivity data.[25,34,35]

Table 2. IR spectral data of HL_1–HL_4 and the complexes of HL_3.

Compound	Frequency /cm^{-1}
HL_1	3389 s[a], 3282 s, 3138 m,br, 1667 m, 1630 m, 1603 m, 1511 m, 1439 s, 1413 m, 1271 s, 1231 m, 1017 m, 915 m, 859 m, 790 m, 736 s, 673 m, 596 m, 438 m
HL_2	3437 m,br, 3284 m, 3179 m,br, 2921 w, 1656 m, 1623 m, 1568 m, 1510 m, 1439 m, 1401 m, 1314 m, 1273 s, 1237 m, 1142 m, 1008 m, 900 m, 845 m, 791 m, 732 m, 653 m, 594 m, 528 m, 436 m
HL_3	3376 m,br, 3293 s, 2938 m, 1628 m, 1591 m, 1538 m, 1482 s, 1425 m, 1385 m, 1256 s, 1057 m, 936 m, 790 m, 733 m, 608 m, 515 m
HL_4	3436 s, 3278 s, 3084 m, 1640 m, 1595 m, 1518s, 1472m, 1388 m, 1334 s, 1276 m, 1247 m, 1071 m, 1000 m, 900 m, 796 m, 740 m, 649 m, 599 m, 553m, 436m
[A] [b]	3406 m,br, 3254 m,br, 3114 m,br, 1635 m, 1613 m, 1563 m, 1534 m, 1480 m, 1385 s, 1284 m, 1239 m, 1070 m, 1025 m, 928 m, 813 m, 718 m, 680 m, 599 m, 493 m
[B]	3550–3100 m,br, 1626 m, 1613 sh, 1559 m, 1475 m, 1429 m, 1384 s, 1284 m, 1236 m, 1213 m, 1103 m, 1065 m, 927 m, 807 m, 723 m, 598 m, 509 m, 473 w
[C]	3453 m,br, 3196 m,br, 1626 m, 1607 m, 1540 m, 1482 m, 1432 m, 1386 s, 1277 m, 1214 m, 1069 m, 1033 m, 944 m, 806 m, 733 m, 598 m
[D]	3600–3100 m,br, 1623 m, 1610 m, 1559 s, 1542 m, 1507 m, 1385 s, 1309 m, 1281 m, 1065 m, 1040 m, 934 m, 805 m, 714 m, 598 m, 487 m

[a] s, strong; m, medium; br, broad; sh, shoulder, w, weak.
[b] [A]:$[Fe(\mathbf{L_3})(OH)(H_2O)_3](NO_3)$;[B]: $[Co(\mathbf{L_3})(H_2O)_2](NO_3)$; [C]: $[Cu(\mathbf{HL_3})(\mathbf{L_3})(H_2O)_2](NO_3)\cdot H_2O$; [D]:$[Zn(\mathbf{L_3})(H_2O)_2](NO_3)$.

Table 3 ^{1}H-NMR spectral data of HL_1–HL_4 and $[Zn(\mathbf{L_3})(H_2O)_2](NO_3)$ (δ_H, ppm; in DMSO-d_6).

Compound	Benzimidazole protons					Phenolic protons				
	H4	H5	H6	H7	NH	H6′	H5′	H4′	OH1	OH2
HL_1	7.65 m [a]	7.27 m	7.27 m	7.65 m	13.01 s,br	6.91 dd 1.6,7.7	6.81 t 7.7,7.8	7.49 dd J = 7.6,1.5	9.22 s,br	13.01 s,br
HL_2	7.56 s,br	2.45 [b] s	7.46 dd J = 1.5,7.8	7.38 s,br	12.98 s,br	6.89 dd J = 8.3,1.5	6.81 t J = 7.8,8.3	7.10 d,br J = 7.3	9.08 s,br	12.98 s,br
HL_3 (isomer A)	7.80 s,br	—	7.49 dd J = 1.5,8.3	7.61 s,br	13.27 s,br	6.92 dd J = 1.5,7.8	6.84 t J = 7.8,8.3	7.30 s,br	9.2 s	12.78 s,br
HL_3 (isomer B)	7.49 dd J = 1.5,8.3	7.61 s,br	—	7.72 s,br	13.27 s,br	6.92 dd J = 1.5,7.8	6.84 t J = 7.8,8.3	7.30 s,br	9.2 s	12.78 s,br
HL_4	8.56 s	—	8.18 d J = 8.8	7.82 d,br	13.61 s,br	6.97 d J = 7.6	6.86 dd J = 7.6,7.6	7.54 d J = 7.6	9.41 s	12.35 s,br
[A] [c]	7.89 s,br	—	7.56 s,br	7.86 d,br J = 5.8	13.21 s	7.31 m,br	7.31 m,br	7.52 d J = 8.3	8.63 s,br	—

[a] s, singlet; d, doublet; dd, doublet of doublet; m, multiplet; br, broad.
[b] 3H (CH_3).[c][A]: $[Zn(\mathbf{L_3})(H_2O)_2](NO_3)$.

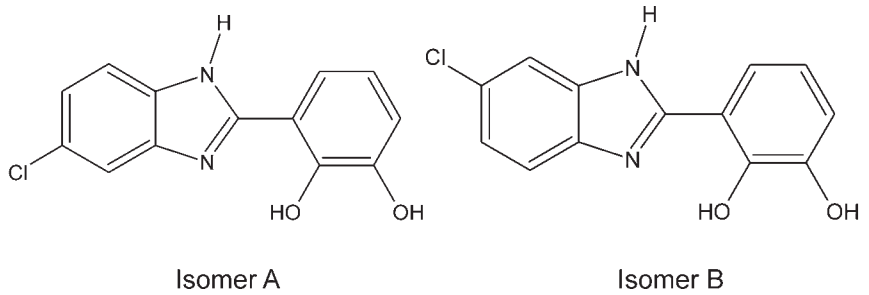

Figure 2 Isomeric structural representation for HL_3 ligand.

3.4. NMR Spectra

The ^{1}H- and ^{13}C-NMR spectral data of the ligands and $[Zn(\mathbf{L_3})(H_2O)_2](NO_3)$ complex are given in Tables 3 and 4, respectively. The OH proton at 1′-position (OH1) appears between 9.08 and 9.41 ppm in the ligands. The OH2 (at 2′-position) and NH protons show broad singlets in the spectra of HL_1, HL_2 and HL_4. This situation is due to the strong intramolecular hydrogen bonding between the C = N nitrogen and phenolic hydrogen atoms. However, the OH2 and NH protons of HL_3 appear separately in the NMR spectrum probably due to two isomeric structures as shown in Fig. 2. The isomeric structures are observed for the benzimidazole protons only (Fig. 3 and Table 3). The integration value of the broad signals at 7.72 and 7.80 ppm show that each of them corresponds to 0.5 protons. These signals can be attributed to H7 (isomer B) and H4 (isomer A) protons, respectively.[36]

Benzimidazole benzene ring protons appear in the 6.81–8.56 ppm range. In the ^{1}H-NMR spectrum of HL_1, two doublets of doublets of AA′XX′ system at δ_H 7.65 (2H) and 7.27 (2H) ppm are attributed for the benzimidazole benzene ring protons.

There are considerable differences between HL_4 and the other benzimidazole derivatives in terms of benzimidazole protons in the ^{1}H-NMR spectra because of the nitro group's strong withdrawing effect. For example, H4 appears at 8.56 ppm (this value is 7.80, 7.65 and 7.56 ppm for HL_3, HL_1 and HL_2, respectively). The other benzimidazole protons (H3, H5 and H6) and NH proton of HL_4 exhibit different chemical shift values to those of the other ligands.

In the ^{1}H-NMR spectrum of the Zn(II) complex, some prominent changes are observed in the characteristics of the phenolic and benzimidazole benzene ring protons with respect to the ligand. For instance, two doublets of doublets (7.49 and 6.92 ppm) and the singlet (9.20 ppm) coalesce to broad singlet, whereas the triplet at 6.84 ppm of the ligand turns into a broad multiplet because of strong metal ion's perturbing effect. On the other hand, the broad singlet at 13.27 ppm for the NH proton in the spectra of HL_3 changed to a singlet (13.21 ppm) in the complex probably due to removing of the intramolecular hydrogen

Table 4. ^{13}C-NMR (APT) spectral data of HL_1–HL_4 and $[Zn(\mathbf{L_3})(H_2O)_2](NO_3)$ (δ_C, ppm; in DMSO-d_6).

Compound	Quaternary carbons	H-bonded carbons
HL_1	152.7, 147.6, 146.8, 113.1	119.4, 117.9, 116.7
HL_2	147.7, 146.9, 113.4	119.5, 117.9, 116.7, 22.0 [a]
HL_3	154.1, 147.7, 147.0, 127.8, 113.2	123.7, 119.7, 119.5, 118.4, 117.1
HL_4	156.8, 147.8, 147.1, 143.7, 113.1	120.0, 119.1, 118.9, 117.8
$[Zn(\mathbf{L_3})(H_2O)_2](NO_3)$	168.3, 163.8, 130.7, 96.8	125.0, 116.2

[a] CH_3.

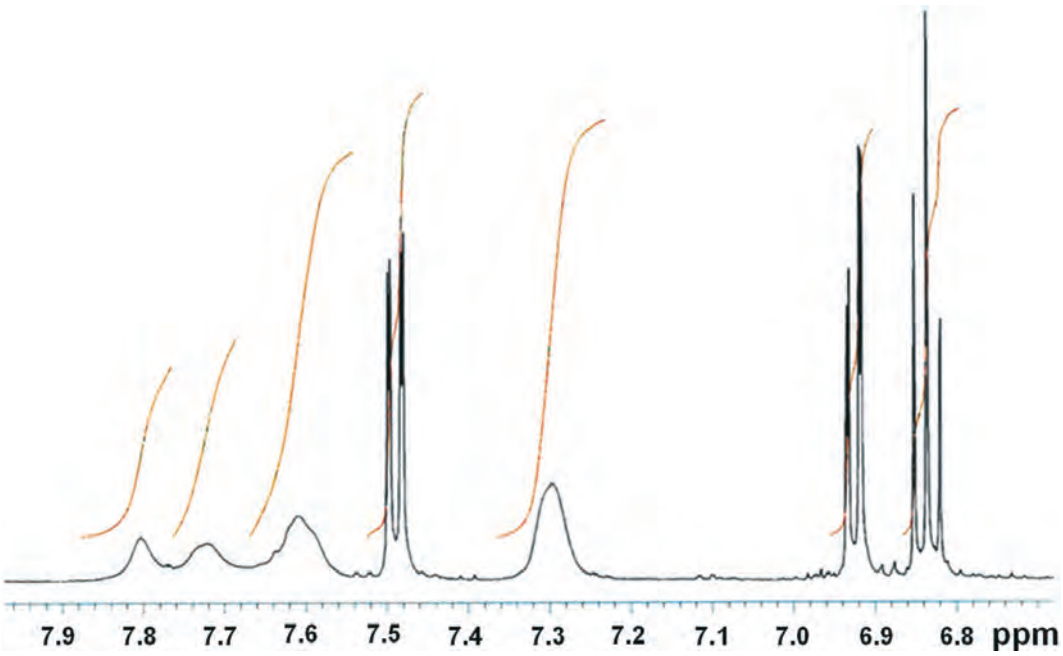

Figure 3 ^{1}H-NMR spectrum of HL_3 between 6.7 and 7.9 ppm (aromatic region) showing isomerism.

bonding as a result of the complexation. The broad singlet at 8.63 ppm belongs to OH1 in the complex spectrum, which appears at 9.20 ppm in the spectrum of the ligand. The OH2 proton's signal in the ^{1}H-NMR spectrum of the Zn(II) complex is removed as expected. This observation is evidence of the OH hydrogen's eliminating and the phenolic oxygen's coordinating to the Zn(II) ion.

In the APT spectra of the ligands all of the carbons could not be detected. However, assignment of some signals could be made: The signals above 150 ppm may be assigned to the C2 carbon atom which is attached to the two imidazole nitrogen atoms (N = C–N).[16–18,37] The signals around 147 ppm in the ligands are attributed to the C1′ and C2′ atoms which are bonded to the OH groups.[38–40]

Good quality NMR spectra for the $[Zn(\mathbf{L_3})(H_2O)_2](NO_3)$ complex could not be recorded because of its very low solubility in DMSO-d_6 and in other polar solvents such as methanol and DMF. This property may be considered as evidence for a polymeric structure.

3.5. Mass Spectra

The ESI-MS spectral data of HL_3 and its complexes are given in Table 5 as molecular ions with the relative abundance.

It is known that chlorine, bromine and copper have two isotopes: These isotopes, their percent abundance and approximately relative proportions are: ^{35}Cl(75.8 %): ^{37}Cl(24.2 %) (3:1); ^{79}Br(50.7 %): ^{81}Br(49.3 %) (1:1); ^{63}Cu(69.2 %): ^{65}Cu(30.8 %) (2:1). On the other hand, zinc has five [^{64}Zn(48.63 %); ^{66}Zn(27.90 %); ^{67}Zn(4.10 %); ^{68}Zn (18.75 %); ^{70}Zn(0.62 %)] and iron has four isotopes [^{54}Fe (5.84 %); ^{56}Fe(91.75 %); ^{57}Fe(2.12 %); ^{58}Fe(0.28 %)] whereas only one isotope is known for cobalt (^{59}Co).

A series of isotopic patterns were identified for the metal complexes of HL_3 due to various isotopes of the chlorine and the central atoms in the complexes (except cobalt). For example, in the mass spectra of $[Zn(\mathbf{L_3})(H_2O)_2](NO_3)$ complex, six isotopic patterns are observed for the molecular ion (Table 5). On the other hand, two significant peaks appear in the spectra of Fe(III) complex for the molecular ion, as expected. These two isotopic patterns arise entirely from chlorine atoms although iron has four isotopes: ^{56}Fe (with 91.75 % relative abundance) is a unique dominant isotope among of isotopes of iron. Since the percentage of the other three isotopes is insignificant.

Ligand peaks are easily seen in the mass spectra of the complexes (the ligand is shown as L_3 in Table 5).

3.6. Thermogravimetric Analyses

The major features of the thermal analysis of the complexes are summarized in Table 6. TGA curves of the complexes are shown

Table 5. ESI-MS spectral data of HL_3 and its complexes.

Compound and MW (g/mol)	Molecular ions (m/z) with relative abundance (%) and isotopic patterns
HL_3 260.7	259.2 (100, $[M-2]^+$ {^{35}Cl}), 260.3 (11.0, $[M]^+$, {^{35}Cl+^{37}Cl}), 261.2 (26.6, $[M+1]^+$ {^{37}Cl}), 262.2 (3.6, $[M+2]^+$)
$[Fe(\mathbf{L_3})(OH)(H_2O)_3](NO_3)$ 448.6	450.4 (6.9, $[M+2]^+$), 452.3 (3.2, $[M+4]^+$), 350.2 (100, $[M-NO_3-3H_2O]^+$), 258.1 ($[M_{L3}-3]^+$)
$[Co(\mathbf{L_3})(H_2O)_2](NO_3)$ 416.6	412.4 (36.2, $[M-4]^+$ {^{37}Cl}), 414.6 (100, $[M-2]^+$ {^{35}Cl}), 416.7 (19.2, $[M]^+$), 354.6 (43.4, $[M-NO_3]^+$), 338.4 (28.4, $[M-NO_3-H_2O-2]^+$), 261.1 (19.2, $[M_{L3}]^+$)
$[Cu(\mathbf{HL_3})(\mathbf{L_3})(H_2O)_2](NO_3)\cdot H_2O$; 698.9	722.3 (100, $[M+23]^+$), 723.2 (49.3, $[M+23+1]^+$), 724.3 (12.2, $[M+23+2]^+$), 663.9 (44.0, $[M-2H_2O]^+$), 261.2 (13.9, $[M_{L3}]^+$)
$[Zn(\mathbf{L_3})(H_2O)_2](NO_3)$ 423.1	421.6 (9.1, $[M-2]^+$), 422.8 (7.3, $[M-1]^+$), 423.6 (7.1, $[M]^+$), 424.4 (6.8, $[M+1]^+$); 425.3 (5.2, $[M+2]^+$), 426.2 (4.3, $[M+3]^+$), 361.3 (100, $[M-H_2O-NO_3]^+$), 259.7 (63.7, $[M_{L3}-2]^+$)

Table 6 TGA data of the complexes (thermal decomposition).

Temperature (°C) →	100	150	200	250	300	350	400	450	500	550	600	>650
Complex						Weight loss (%)						
[A] [a]	1.9	5.6	12.0	53.5	54.7	72.6	78.1	80.5	80.8	81.2	81.7	82.3
[B]	2.0	5.2	11.7	8.3	23.2	29.1	37.7	50.1	59.0	72.5	83.7	84.1
[C]	2.3	7.0	12.2	18.5	22.5	27.3	34.5	46.9	56.4	77.1	87.5	87.7
[D]	2.1	7.7	10.0	12.6	18.3	28.6	36.2	43.8	57.9	68.2	80.7	83.4

[a] [A], $[Fe(\mathbf{L_3})(OH)(H_2O)_3](NO_3)$; [B], $[Co(\mathbf{L_3})(H_2O)_2](NO_3)$; [C], $[Cu(\mathbf{HL_3})(\mathbf{L_3})(H_2O)_2](NO_3)\cdot H_2O$; [D], $[Zn(\mathbf{L_3})(H_2O)_2](NO_3)$.

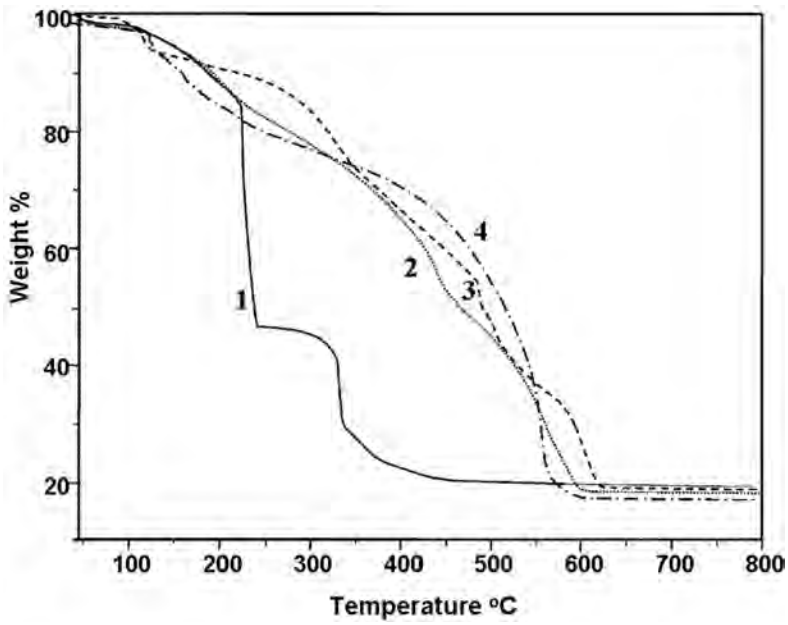

Figure 4 TGA curves of the complexes: 1: $[Fe(\mathbf{L_3})(OH)(H_2O)_3](NO_3)$; 2: $[Co(\mathbf{L_3})(H_2O)_2](NO_3)$; 3: $[Zn(\mathbf{L_3})(H_2O)_2](NO_3)$; 4: $[Cu(\mathbf{HL_3})(\mathbf{L_3})(H_2O)_2](NO_3)\cdot H_2O$.

in Fig. 4. The samples of the complexes were heated from room temperature up to 800 °C. Thermal analysis results exhibited the valuable information about the water coordination state of the complexes.

In the TG analysis of Co(II), Zn(II) and Fe(III) complexes there is no significant weight loss until 120 °C; above 120 °C, the weight losses being between 5.2–7.7 %. This finding serves as proof of the nonexistence of uncoordinated water molecule in the mentioned complexes. These findings are in line with the mass and elemental analysis of the complexes. The coordinated water molecules are removed from Fe(III), Co(II) and Zn(II) complexes at temperatures between 110 and 150 °C.[41,42] The weight loss of 2.3 % for the Cu(II) complex below 100 °C corresponds to one mole of uncoordinated lattice water (Table 6, first column). Calculated percentage of one mole of water is 2.5 % for the Cu(II) complex.

The sharp drop observed (weight loss of 38 %) in the 220–240 °C range of the TGA curve of the Fe(III) complex is considerably different from the other complexes. This difference can be explained by the Fe(III) complex having a trivalent metal ion. Fe(III) ion may be reduced easily by heating and begins to decompose earlier than the others. The weight loss at this stage can be explained in terms of the cleavage of the chlorine atom, hydroxo and hydroxy groups and also as decomposition of nitrate ion. Fe(III) complex above 400 °C and the others above 600 °C decompose to metal oxide, carbon dioxide and water. The metal percentages of the complexes are calculated from the residual percentage of metal oxide % formed in the final step and are in good agreement with data obtained by the wet combustion method of MacDonald.[42,43]

According to the TGA data, two water molecules coordinate to the Cu(II) ion in $[Cu(\mathbf{HL_3})(\mathbf{L_3})(H_2O)_2](NO_3)\cdot H_2O$. This complex contains an uncoordinated water molecule, also. The presence of a nitrate ion shows that OH1 hydrogen atom did not eliminate from the second HL_3 ligand of the Cu(II) complex. Namely, it may be concluded that Cu(II) complex is a penta-coordinated complex as depicted in Fig. 5 and in the literature.[9]

3.7. Fluorescence Spectra

Excitation and emission spectra of the compounds were obtained in ethanol solution at room temperature (excitation wavelength: 354 nm; concentration: 10^{-4} M). The emission spectral data are presented in Table 7. The fluorescence spectra of all the compounds in the study are shown in Fig. 6.

HL_1 shows a strong emission band at 479 nm with a shoulder at 395 nm. The other ligands also have two emission bands, a main band and a shoulder or weak band (at the lower wavelength) (Table 7). Based on the excited state intramolecular proton transfer (ESPT) theory, the fluorescence band at the lower wavelength is attributed to the emission from the enol form of the ligands, while the band at the higher wavelength is attributed to the emission from the keto form of the ligands *via* an ESPT process (Fig. 7). According to the ESPT process, it is possible to say that all of the ligands exist in the keto form in ethanol.

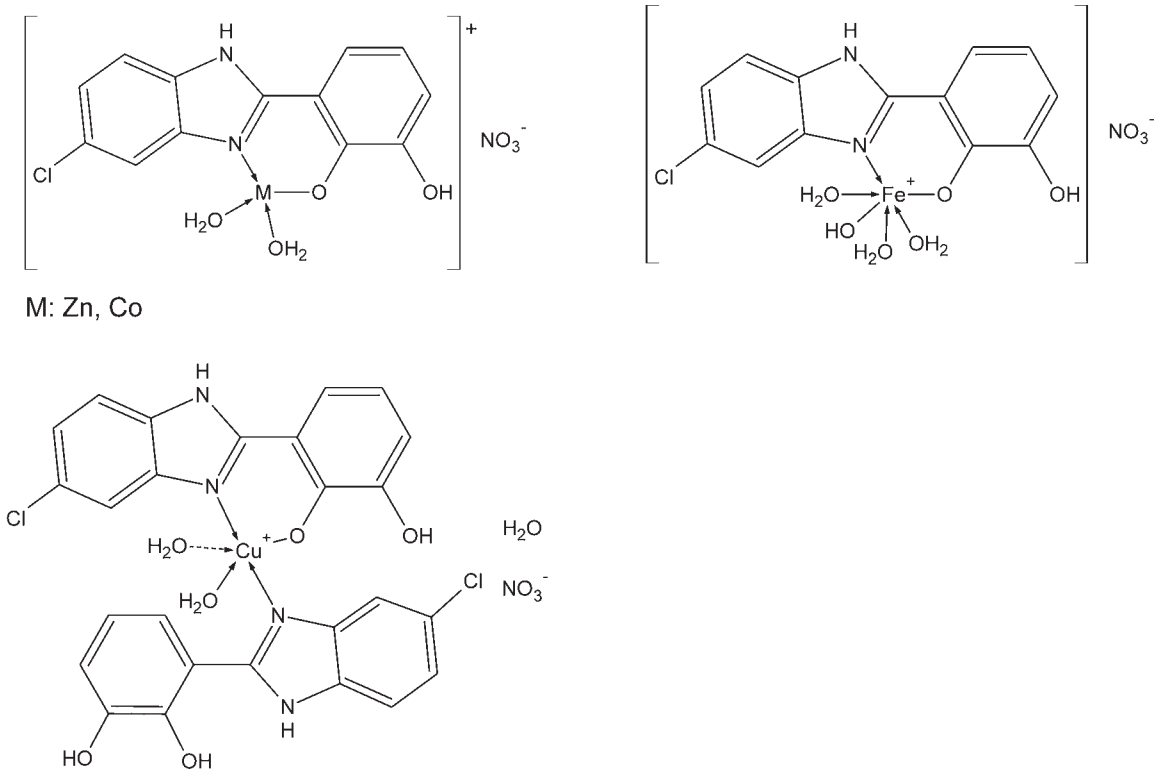

Figure 5 The proposed structural representation for the studied complexes.

Table 7 Emission maximum wavelengths (nm) of the compounds.

Compound	Emission maximum	Compound	Emission maximum
HL_1	395 sh, 479 s [a]	$[Fe(\mathbf{L_3})(OH)(H_2O)_3](NO_3)$	394 w, 430 w
HL_2	394 sh, 475 s	$[Co(\mathbf{L_3})(H_2O)_2](NO_3)$	378 sh, 452 s
HL_3	394 w, 489 s	$[Cu(\mathbf{HL_3})(\mathbf{L_3})(H_2O)_2](NO_3)\cdot H_2O$	392 sh, 438 w
HL_4	393 w, 461 m	$[Zn(\mathbf{L_3})(H_2O)_2](NO_3)$	393 w, 440 w

[a] s, strong; m, medium; w, weak.

The fluorescence band maximum of HL_3 is red-shifted with respect to that of HL_1; whereas the others are blue-shifted under UV radiation. Different photophysical behaviour is observed for HL_3 (chloro derivative). The longer emission wavelength as compared to the other benzimidazolyl-phenols indicates this ligand has more extensive conjugation between the two rings.[44,45] All of the HL_3 complexes show a blue shift in the fluorescence spectra as compared to the free ligand. It is interesting that the Co(II) complex shows strong fluorescence at 452 nm whereas the other complexes emit weak fluorescence near 430 nm.This emission nature can be attributed to the ligand-centred charge transfer transition (LCCT) with $\pi \rightarrow \pi^*$ property.[46]

All of the compounds are fluorescent in the visible region. Thus, these compounds have potential applications as luminescent materials in light-emitting devices.

3.8. Antimicrobial Activity

The results concerning *in vitro* antimicrobial activity of the ligands and the complexes together with MIC values of known antibiotics and antifungal reagents are presented in Table 8.

It is observed that HL_1, HL_2, HL_3 and $[Cu(\mathbf{HL_3})(\mathbf{L_3})(H_2O)_2](NO_3)\cdot H_2O$ exhibit moderate antifungal activity toward *C. albicans*. In addition, these four compounds show very weak antibacterial activity against *S. epidermidis* (Gram+ bacteria). The latter two compounds, HL_3 and its Cu(II) complex, are also weakly effective against *S. aureus* (Gram+). HL_3 exhibits a broader spectrum of antimicrobial activity as compared to the other compounds. HL_4, nitro derivative, has no activity toward the microorganisms (not reported). This situation can be related with the H-bonding in the ligands: HL_1, HL_2 and HL_3, which have relatively weaker H-bonding as compared to HL_4 (see IR Spectra Section), show weak antimicrobial activity. According to this observation, there may be a relation between hydrogen bonding and antimicrobial activity of the ligands.

It is observed that the Cu(II) complex of HL_3 has very weak

Table 8. *In vitro* antimicrobial activity of the compounds and the standard reagents (MIC, μg mL^{-1}).

Compound	Microorganisms		
	Sa [a]	*Se*	*Ca*
HL_1	– [b]	625	39
HL_2	–	312	9.8
HL_3	312	312	9.8
[C] [c]	625	625	19.5
Ciprofloxazin	0.125	156	–
Cefuroxime Na	–	9.8	–
Fluconazole	–	–	1.0

[a] *Sa, Staphylococcus aureus* ATCC 6538; *Se, Staphylococcus epidermidis* ATCC 12228; *Ca, Candida albicans* ATCC 10231.
[b] –: High MIC values (>625 μg mL^{-1}).
[c] [C]: $[Cu(\mathbf{HL_3})(\mathbf{L_3})(H_2O)_2](NO_3)\cdot H_2O$.

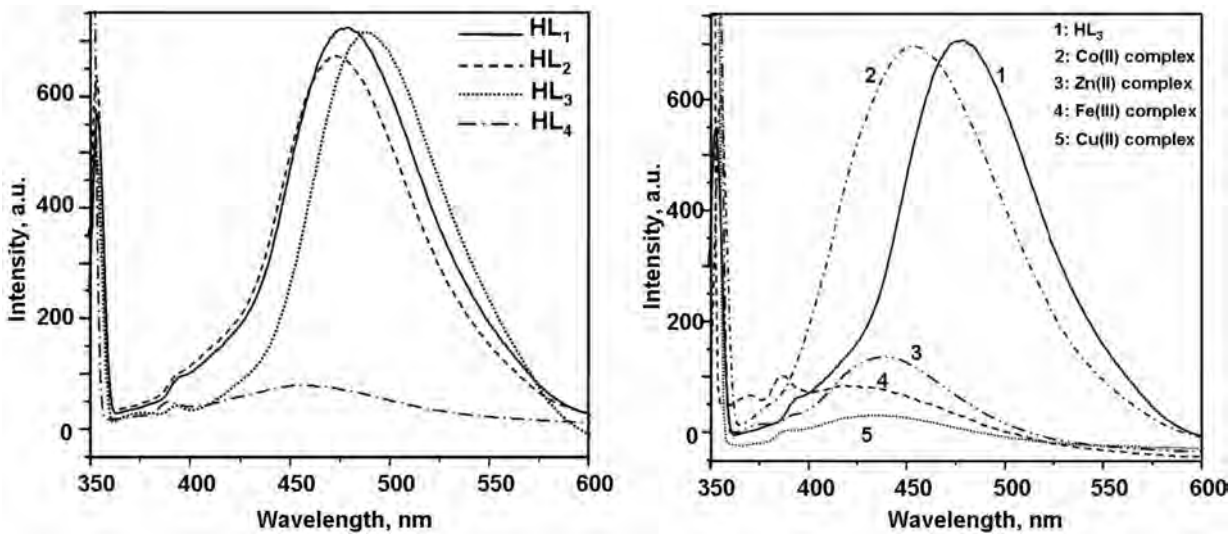

Figure 6 Fluorescence spectra of the compounds in the study at room temperature in methanol.

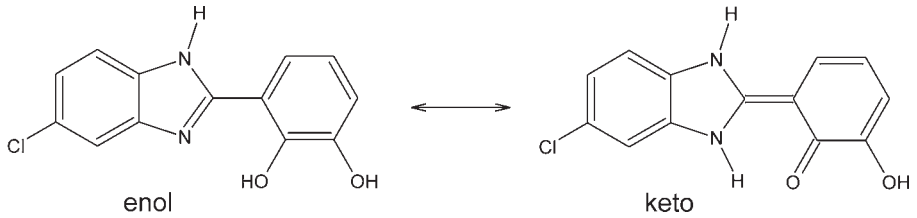

Figure 7 Enol-keto tautomerism for HL_3.

antibacterial activity and moderate antifungal activity, while the other complexes are inactive. On the other hand, it should be noted that the metal salts $Fe(NO_3)_3$, $Cu(NO_3)_2$, $Co(NO_3)_2$ and $Zn(NO_3)_2$ did not show any effect on the microorganisms.

4. Conclusions

Benzimidazolyl-phenols are potential N, O donors and they react easily with metal ions to give stable chelate complexes. In this study, 3-(5-H/Me/Cl/NO_2-1*H*-benzimidazol-2-yl)-benzene-1,2-diols (HL_X; X = 1–4) and HL_3 complexes with $Fe(NO_3)_3$, $Cu(NO_3)_2$, $Co(NO_3)_2$, $Zn(NO_3)_2$ have been synthesized and characterized. All of the complexes fluoresce with the Co(II) complex showing the highest fluorescence intensity, and higher emission wavelength. Antibacterial activities of the ligands and the complexes were evaluated using the disk diffusion method against *Staphylococcus aureus ATCC 6538, Staphylococcus epidermidis ATCC 12228, Escherichia coli ATCC 8739, Klebsiella pneumoniae ATCC 4352, Pseudomonas aeruginosa ATCC 27853, Proteus mirabilis ATCC 14153* and *Candida albicans.* It is observed that HL_3 exhibits a broader spectrum of antimicrobial activity as compared to the other compounds. HL_1, HL_2, HL_3 and $[Cu(\mathbf{HL_3})(\mathbf{L_3})(H_2O)_2](NO_3)\cdot H_2O$ exhibit moderate antifungal activity toward *C. albicans* and show very weak antibacterial activity against *S. epidermidis* (Gram+ bacteria).

Acknowledgements

This work was supported by the Istanbul University Research Fund and TUBITAK (The Scientific and Technological Research Council of Turkey). COST project number: TBAG-U/185 (106T086).

References

1 T.J. Lane, I. Nakagawa, J.L. Walter and A.J. Kandathil, *Inorg. Chem.*1962, **1**, 267–276.

2 D.H. Verkhovodova, N.R. Kal'nitskii, V.I. Minkin, A.D. Garnovskii and O.A. Osipov, *Zh. Neorg. Khim.*1967, **12**, 3385–3387; C.A. 1968, **68**, 83943n.

3 S.K. Gupta and L.K. Mishra, *J. Inorg. Nucl. Chem.*1979, **41**, 890–891.

4 A. Mishra, M.P. Singh and J.P. Singh, *J. Indian Chem. Soc.* 1980, **57**, 246–251; A. Mishra, V.K. Singh, *J. Indian Chem. Soc.* 1981, **58**, 122–124; L.K. Mishra, *J. Indian Chem. Soc.* 1982, **59**, 408–409.

5 C.G. Wahlgren, A.W. Addison, S. Burman, L.K. Thompson, E. Sinn and T.M. Rowe, *Inorg. Chim. Acta* 1989, **166**, 59–69.

6 M.R. Maurya and S.A. Bhakare, *J. Chem. Res., Synop.* 1996, **8**, 390–391; C.A. 1996, **125**, 264182e.

7 A. Tavman and B. Ülküseven, *Main Group Met. Chem.* 2001, **24**, 205–210; B. Ülküseven, A. Tavman, G. Ötük and S. Birteksöz, *Folia Microbiol.* 2002, **47**, 481–487.

8 Y.-P. Tong, *Acta Cryst.* 2005, **E61**, m1595–m1597.

9 Y.-P. Tong and B.-H. Ye, *Acta Cryst.* 2004, **E60**, m1927–m1929.

10 Y. Xi, J. Li and F. Zhang, *Acta Cryst.* 2005, **E61**, m1953–m1954.

11 H.-Y. Bu, Y.-J. Liu, Q.-F. Liu and J.-F. Jia, *Acta Cryst.* 2005, **E61**, m1986–m1987.

12 Y.-H. Zhao, Z.-M. Su, Y. Wang, X.-R. Hao and K.-Z. Shao, *Acta Cryst.* 2006, **E62**, m2361–m2362.

13 A. Tavman, N.M. Agh-Atabay, A. Neshat, F. Gücin, B. Dülger and D. Haciu, *Transit. Met. Chem.* 2006, **31**, 194–200.

14 Y.P. Tong and S.L. Zheng, *J. Mol. Struct.* 2007, **841**, 34–40.

15 Q. Shi, S. Zhang, F. Chang, P. Hao and W.-H. Sun, *C. R. Chimie,* 2007, **10**, 1200–1208.

16 A. Tavman, S. Ikiz, A.F. Bagcigil, Y.N. Ozgür and S. Ak, *J. Serb. Chem. Soc.* 2009, **74**, 537–548.

17 A. Tavman, S. Ikiz, A.F. Bagcigil, Y.N. Ozgür and S. Ak, *Turk. J. Chem.* 2009, **33**, 321–331.

18 A. Tavman, S. Ikiz, A.F. Bagcigil, Y.N. Ozgür and S. Ak, *Russ. J. Inorg. Chem.* 2010, **55**, 215–222.

19 A. Tavman, I.Boz, A.S. Birteksöz and A. Cinarli, *J. Coord. Chem.* 2010, **63**, 1398–1410.

20 A. Tavman, N.M. Agh-Atabay, S. Güner, F. Gucin and B. Dülger, *Transit. Met. Chem.* 2007, **32**, 172–179.

21 A. Tavman, I. Boz and A.S. Birteksöz, *Spectrochim. Acta* 2010, **A77**, 199–206.

22 H.F. Ridley, G.W. Spickett and G.M. Timmis, *J. Het. Chem.*1965, **2**, 453–456.

23 Clinical and Laboratory Standards Institute (CLSI). Methods for dilution antimicrobial susceptibility tests for bacteria that grow aerobically, Approved Standard M7–A5, Wayne, PA, 2006.

24 Clinical and Laboratory Standards Institute (CLSI). Reference method for broth dilution antifungal susceptibility testing of yeasts, Approved Standard M27-A2, Wayne, PA, 2002.

25 A. Tavman, *Spectrochim. Acta* 2006, **A63**, 343–348.

26 M. Masoud, A.E. Ali, M.A. Shaker and M.A. Ghani, *Spectrochim. Acta* 2005, **A61**, 3102–3107.

27 S. Chandra, X. Sangeetika and S.D. Sharma, *Spectrochim. Acta* 2003, **A59**, 755–760.

28 S. Padhye and G.B. Kauffman, *Coord. Chem. Rev.* 1985, **63**, 127–160.

29 A.K. El-Sawaf, D.X. West, R.M. El-Bahnasawy and F.A. El-Saied, *Transit. Met. Chem.*1998, **23**, 227–232.

30 R.K. Agarwal, D. Sharma, L. Singh and H. Agarwal, *Bioinorg. Chem. Appl.* 2006, **2006**, 1–9.

31 D. Kanamori, Y. Yamada, A. Onoda, T.A. Okamora, S. Adachi, H. Yamamoto and N. Ueyama, *Inorg. Chim. Acta* 2005, **358**, 331–338.

32 N. Ueyama, N. Nishikava, Y. Yamada, T. Okamura and A. Nakamura, *Inorg. Chim. Acta* 1998, **283**, 91–97.

33 V.M. Leovac, L.S. Jovanovic, V.S. Cesljevic, L.J. Bjelica, V.B. Arion and N.V. Gerbeleu, *Polyhedron* 1994, **13**, 3005–3014.

34 K. Nakamoto, *Infrared and Raman Spectra of Inorganic and Coordination Compounds, Part B,* 5th edn., John Wiley & Sons, New York, 1997.

35 D.Y. Kong and Y.Y. Xie, *Polyhedron* 2000, **19**, 1527–1537.

36 N.E. Eltayeb, S.G. Teoh, R. Adnan, H.-K. Fun and S. Chantrapromma, *Acta Cryst.* 2009, **E65**, o3227–o3228.

37 A. Tavman, B. Ulküseven and N.M. Agh-Atabay, *Transit. Met. Chem.* 2000, **25**, 324–328.

38 A. Mikolasch, E. Hammer, U. Jonas, K. Popowski, A. Stielow and F. Schauer, *Tetrahedron* 2002, **58**, 7589–7593.

39 C. Lee, J. Kim, H. Lee, S. Lee and Y. Kho, *J. Nat. Prod.* 2001, **64**, 659–660.

40 V.V. Barbakadze, E.P. Kemertelidze, I. Targamadze, K. Mulkidzhanyan, J. Kemink, A.J. J. van den Berg, K.J. Beukelman and A.I. Usov, *Chem. Nat. Comp.* 2005, **41**, 374–377.

41. K.K.M. Yusuff and R. Sreekala, *Thermochim. Acta,* 1991, **179**, 313–322.

42. A.A. Soliman and W. Linert, *Thermochim. Acta* 1999, **338**, 67–75.

43. A.M.G. MacDonald and P. Sirichanya, *Microchem. J.* 1969, **14**, 199–206.

44. C. Mukhopadhyay, S. Ghosh and R.J. Butcher, *Arkivoc,* 2010, **9**, 75–96.

45. L.M. Dudd, E. Venardou, E. Garcia-Verdugo, P. Licence, A.J. Blake, C. Wilson and M. Poliakoff, *Green Chem.* 2003, **5**, 187–192.

46 Y.-P. Tong and Y.-W. Lin, *J. Chem. Crystallogr.* 2008, **38**, 613–617.